References and Notes

1. W. H. K. Lee and S. Uyeda, in *Terrestrial Heat Flow*, W. H. K. Lee, Ed. (American Geophysical Union, Washington, D.C., 1965), p. 87.
2. J. G. Sclater and J. Francheteau, *Geophys. J. R. Astron. Soc.* **20**, 509 (1970).
3. W. M. Kaula, *Science* **169**, 982 (1970); in *The Nature of the Solid Earth*, E. C. Robertson, Ed. (McGraw-Hill, New York, 1972), p. 385; *J. Geophys. Res.* **74**, 4807 (1969); K. Lambeck, *Geophys. J. R. Astron. Soc.* **30**, 37 (1972).
4. J. Dorman, M. Ewing, J. Oliver, *Bull. Seismol. Soc. Am.* **50**, 87 (1960); L. Knopoff, *Tectonophysics* **13**, 497 (1972).
5. H. Kanamori, *Phys. Earth Planet. Interiors* **2**, 259 (1970); A. Dziewonski, *Geophys. J. R. Astron. Soc.* **22**, 289 (1971).
6. M. N. Toksöz and D. L. Anderson, *J. Geophys. Res.* **71**, 1649 (1966).
7. R. Madariaga and K. Aki, *ibid.* **77**, 4421 (1972).
8. J. N. Brune, J. E Nafe, J. Oliver, *ibid.* **65**, 287 (1960).
9. L. Knopoff and F. A. Schwab, *ibid.* **73**, 755 (1968).
10. F. A. Schwab and L. Knopoff, in *Methods in Computational Physics*, B. A. Bolt, Ed. (Academic Press, New York, 1972), vol. 11, p. 87.
11. R. Burridge and L. Knopoff, *Bull. Seismol. Soc. Am.* **54**, 1875 (1964).
12. E. Herron, in *Antarctic Oceanology I*, vol. 15 in *Antarctic Research Series*, J. L. Reid, Ed. (American Geophysical Union, Washington, D.C., 1971), p. 229; R. C. Larson and C. G. Chase, *Geol. Soc. Am. Bull.* **83**, 3627 (1972).
13. A. R. Leeds, L. Knopoff, E. G. Kausel, *Science* **186**, 141 (1974).
14. Phase velocities for path ANP 9 were measured over the period range 100 to 190 seconds.
15. W. Stauder, *J. Geophys. Res.* **73**, 7693 (1968).
16. A. R. Leeds, thesis, University of California, Los Angeles (1973).
17. B. Isacks, L. R. Sykes, J. Oliver, *Geol. Soc. Am. Bull.* **80**, 1443 (1969).
18. P. Molnar and L. R. Sykes, *ibid.*, p. 1639.
19. W. Stauder, *J. Geophys. Res.* **73**, 3847 (1968).
20. L. R. Sykes, *ibid.* **72**, 2131 (1967).
21. C. R. Allen and J. M. Nordquist, *U.S. Geol. Surv. Prof. Pap. 787* (1972), p. 16.
22. T. V. McEvilly, W. M. Bakun, K. B. Casaday, *Bull. Seismol. Soc. Am.* **57**, 1221 (1967).
23. Supported by the Earth Sciences Section, National Science Foundation (grants GA-37119X and GA-18673). Publication No. 1267, Institute of Geophysics and Planetary Physics, University of California, Los Angeles.

* Present address: Department of Geophysics, University of Chile, Santiago.

† Present address: Lamont-Doherty Geological Observatory, Columbia University, Palisades, New York 10964.

20 June 1974

Variations of Upper Mantle Structure under the Pacific Ocean

Abstract. *The inversion of Rayleigh wave dispersion data for the Pacific Ocean shows that lithospheric thickness increases systematically with age. The lid to the low-velocity channel is very thin or absent near the ridge crest; the low-velocity channel may be absent in the oldest parts of the ocean.*

Observations of the dispersion of Rayleigh waves indicate that there is significant heterogeneity in the structure of the upper mantle beneath the Pacific Ocean (*1*). The heterogeneity is sufficiently well correlated with lithospheric age for this to form the most appropriate basis for inversion of the observations at this time. In a sense, the use of lithospheric ages provides one coordinate of a system for the Pacific Ocean. In the absence of any theory for the variation of dispersion in the Pacific, we see no particular reason to use surface harmonic or polynomial expansions of observations (*2*) or indeed to use functions of any coordinate system obtained from geographical considerations as a basis for inversion.

The geophysical inverse problem is a search for a certain class of models; specified mathematical operations on these models yield a set of values which fit the observations within a specified accuracy (*3*). Two methods of analysis can be considered for the inverse problem. In the most popular procedure, the observations of dispersion on paths crossing a large area are decomposed into regional dispersion relations, which can then be inverted to give local structure (*2, 4, 5*). However, this procedure may mask the fact that models constructed for one region depend interactively on models constructed for other regions. The construction of regionalized dispersion curves may generate a data base with apparently more degrees of freedom than are present in the original data set. In the case of a system with only 5 degrees of freedom in the original dispersion data, one would not be able to adjust the 16 parameters of lid and channel thickness and velocity in each of four geographic regions independently; however, the construction of regionalized dispersion curves from the original data set might give the illusion that 4 degrees of freedom were present in each of the dispersion curves.

Table 1. Regionalized lithospheric ages and lengths of paths.

Region	Average age (million years)	Total path length (km)
1	150	26309
2	120	18716
3	100	60716
4	70	34872
5	50	44884
6	30	39455
7	15	19295
8	5	23278

In the method of analysis we used, the dispersion measurements are inverted directly into regional upper mantle structures; the interplay of regional structural parameters is adjusted so that the sums of the phase delays across each region match the observations in an appropriate manner. The regional dispersion relations can then be derived from the regional structure.

We used a subdivision of the Pacific Basin into eight zones, each having a different value of lithospheric age (*6*) (Table 1), plus a ninth zone which represents the marginal seas behind island arcs. The first eight regions represent a subdivision of the tectonic history of the upper mantle of the Pacific from ridge to trench. The input data were 182 Rayleigh wave phase velocities, sampled at selected periods from 30 seconds to the longest periods available, for 31 paths; the longest period used was 190 seconds. The total length of the paths traversing each age region is given in Table 1. Since a significant fraction of the total path length is spent in region 9, independent measurements were made of phase velocities for four paths wholly in the marginal seas and were used to correct the phase velocities for the 31 paths in the eight regions (*7*). Corrections to the phase velocities were $\lesssim 0.02$ km/sec. Each phase velocity measurement was weighted in the inversion according to the total path length and period, the longer path lengths and shorter periods having the greater weighting factors.

We report results for five related numerical inversion experiments, which differ in the nature of the constraints used in parameterizing the models. Certain features of the parameterization were preserved in all five experiments. The crust and upper mantle were divided into a small number of layers: the water layer, the crust including sediments, the lid to the low-velocity channel, the low-velocity channel, and the subchannel regions. Below the subchannel, and beginning at a depth of ~ 450 km, there is a standard platform (*8*). The lithosphere consists of the crust and the lid, and the asthenosphere is taken to be the low-velocity channel. In each region the thickness of crust and depth of water were chosen to match best local estimates. The *P*-wave velocities (V_P) and densities for the layers were not used as variables, and the *S*-wave velocities (V_S) in the crust and platform were fixed. The *S*-wave velocities in the lid, channel, and subchannel and the depths to the interfaces between these layers

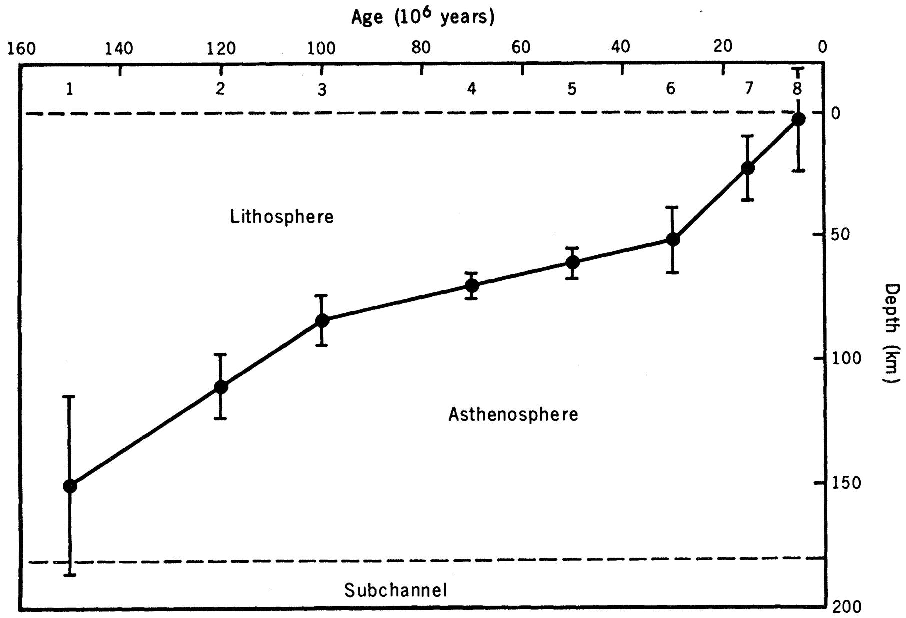

Fig. 1. Variation of upper mantle structure as a function of lithospheric age for the second inversion. Depths are measured from the top of the lithosphere. Region numbers are shown beneath the age scale.

were allowed to vary or were specified.

To reduce the number of parameters involved in the inversion, only the upper mantles under regions 1, 3, 6, and 8 were parameterized. The structures in 2, 4, 5, and 7 were derived from those in the adjoining regions by a linear interpolation by age on the values in regions 1, 3, 6, and 8. This procedure is a compromise between detailed spatial resolution and the small number of structural parameters consistent with our data.

In the first inversion experiment, V_S in the lid was fixed at 4.6 km/sec. The depth to the channel-subchannel interface was fixed at 180 km below sea level with a subchannel V_S of 4.55 km/sec (*8*). The eight parameters used in this inversion were the depth from sea level to the lid-channel interface and the channel velocity in each of the four regions.

A least-squares fit to the input data provides a starting structure for a subsequent detailed inversion. The eight-parameter analysis gave a model in which the lithospheric thickness increased monotonically with age; V_S in the channel varied between 4.0 and 4.2 km/sec in a nonmonotonic way. This range of channel velocities was considered sufficiently narrow that we fixed the channel velocity at 4.1 km/sec in the remaining four numerical experiments.

In the second experiment, V_S in the lid, channel, and subchannel was fixed at 4.6, 4.1, and 4.55 km/sec, respectively, and the depth to the channel-subchannel interface was fixed at 180 km as before. The results of the least-squares fit to the data for this four-parameter experiment is shown in Table 2, along with a list of the other parameters used in the analysis. An Edgehog analysis (*9*) gave the error estimates for the four variable lid thickness parameters as well as the four interpolated lid thicknesses. The least-squares fit and the maximum range of these thicknesses are shown in Fig. 1. The error bars give the extreme values of a regional lid thickness if all four parameters are allowed to vary simultaneously.

The most striking result is that the thickness of the lithosphere in the Pacific Basin grows from a few kilometers in region 8 to well over 100 km in the oldest parts. The span of models includes some in which the low-velocity channel disappears completely beneath the oldest parts, and thus we cannot say whether a low-velocity channel is present in region 1.

The large error bars in region 1 are due to at least two effects; the relatively short overall path length in this region and the dependence of the determination of deep structures on increasingly sparse and uncertain long-period measurements. In addition, the almost zero thickness of lithosphere in the neighborhood of the ridges may be a consequence of assuming a channel velocity of 4.1 km/sec for this region; if the channel velocity were as low as 3.9 or 4.0 km/sec, values which have been suggested (*5, 10*), then a high-velocity lid about 10 to 20 km thick might be appropriate.

Our result shows that the lid grows rapidly in the first 30 million years after its formation, then thickens more gradually, and then apparently grows at an increasing rate again after 100 million years. The division into three straight-line segments in Fig. 1 is arbitrary, and a smooth curve would probably be more plausible. We cannot resolve the nature of the corners at 30 and 100 million years any better than we have. An increase in the number of parameters corresponding to an increase in

Table 2. Regional models.

Layer	Layer thickness (km) in region								Density (g/cm^3)	V_P (km/sec)	V_S (km/sec)
	1	2	3	4	5	6	7	8			
Water	5.8	5.8	5.8	5.4	5.1	4.4	3.8	3.1	1.03	1.52	0
Crust: Sediment	0.3	0.3	0.3	0.2	0.2	0.1	0.1	0	2.00	1.65	1.00
Crust	1.4	1.4	1.4	1.4	1.4	1.4	1.4	1.4	2.60	5.15	3.00
	4.7	4.7	4.7	4.7	4.7	4.7	4.7	4.7	2.90	6.80	3.90
Lid	135	103	81	68	60	51	23	3	3.40	8.10	4.60
Channel	33	65	87	100	109	118	147	168	3.40	7.60	4.10
Subchannel	275	275	275	275	275	275	275	275	3.50	8.20	4.55
Deeper mantle	250	250	250	250	250	250	250	250	3.96	9.80	5.40
	150	150	150	150	150	150	150	150	4.21	10.00	5.90
	∞	∞	∞	∞	∞	∞	∞	∞	4.95	11.48	6.38

the number of chronologic regions merely increases the size of the error bars.

Hart and Press (*11*) have proposed that in the Atlantic the velocity of S_n, the *S*-wave in the lid, varies with age, being 4.58 km/sec in the regions younger than 50 million years and 4.7 km/sec in the regions older than 50 million years. At the epicentral distances used by Hart and Press, S_n travels at the highest *S*-wave velocity within the lid. If the *S*-wave velocity increases with depth in the lid, the body wave observations can be explained while preserving the notion of a constant *S*-wave velocity at the same depth throughout the basin. In our third experiment we allowed the lid density, V_P, and V_S to be linear functions of depth in the lid; the same set of relations was used for the entire Pacific. The increase of properties with depth was abruptly truncated by the start of the channel. The properties of the channel and subchannel were as before. The gradient of V_S in the lid was adjusted to match the values quoted by Hart and Press for the bottom of the lid at 25 and 75 million years. The results of the least-squares inversion gave only small changes from the result of Fig. 1. In the youngest region, the lid is so thin that a new lid velocity does not affect the thickness. At 50 million years (region 5), the average lid velocity is 4.6 km/sec, as in the preceding calculation, and the thickness is the same as in Fig. 1. In any case, the new least-squares fit lies well within the error bars of Fig. 1.

In the fourth calculation, we tested the assumptions regarding the channel-subchannel interface. We continued to assume that the depth to this interface is a constant throughout the Pacific; to make this depth a separate variable in each of the four regions leads to unstable solutions. The other parameters were fixed as before. A least-squares fit to the five-parameter system (four lid thicknesses and the depth to the subchannel) gave a depth to the subchannel of 175 km, virtually identical with the constrained estimate of the second calculation (180 km).

In the fifth inversion experiment we raised V_S in the subchannel to 4.75 km/sec, with the other parameters fixed as in the fourth calculation. The resulting five-parameter fit gave a depth to the subchannel of 207 km, an increase from 180 km. The new lid thicknesses are all within 6 km of the previous values. Thus, an increase in the subchannel velocity can be balanced by a thicker channel and a thinner subchannel without significant change in lid thicknesses.

Raitt (*12*) has stated that anisotropy may be present in the upper mantle of the central Pacific. There is also information bearing on this point from surface waves crossing the Nazca plate in a relatively dense pattern of paths (*5*). Unfortunately, with the present data we cannot distinguish between anisotropy and a more detailed regional variation in structure. The introduction of anisotropy (or additional isotropic layers) as an additional model parameter could not worsen the fit, but would lead to increased instability in the solution.

Inversions of these surface wave observations are incapable of giving simultaneous determinations of lid and channel velocity and thickness, plus anisotropy, as a function of age. However, any reasonable assumption leads to the result that the lid is very thin or absent near the ridge crest. The lid must thicken with age, reaching a thickness of about 60 km after 50 million years and about 85 km after 100 million years. After this age the lid continues to grow, although the thickness we get depends sensitively on the assumptions we make.

ALAN R. LEEDS*
LEON KNOPOFF, EDGAR G. KAUSEL†
Institute of Geophysics and Planetary Physics, University of California, Los Angeles 90024

References and Notes

1. E. G. Kausel, A. R. Leeds, L. Knopoff, *Science* **186**, 139 (1974).
2. J. C. Savage and W. R. H. White, *Can. J. Earth Sci.* **6**, 1289 (1969).
3. G. Backus and F. Gilbert, *Geophys. J. R. Astron. Soc.* **16**, 169 (1968); *Phil. Trans. R. Soc. Lond. Ser. A* **266**, 123 (1970); D. D. Jackson, *Geophys. J. R. Astron. Soc.* **28**, 97 (1972); L. Knopoff and D. D. Jackson, in *Dynamic Response of Structures*, G. Herrmann and N. Perrone, Eds. (Pergamon, New York, 1972), p. 289.
4. T. Santô, *Bull. Earthquake Res. Inst.* **41**, 719 (1963); H. Kanamori, *Phys. Earth Planet. Interiors* **2**, 259 (1970); D. L. Anderson and M. N. Toksöz, *J. Geophys. Res.* **71**, 1649 (1966).
5. D. W. Forsyth, thesis, Massachusetts Institute of Technology (1973).
6. J. G. Sclater and J. Francheteau, *Geophys. J. K. Astron. Soc.* **20**, 509 (1970); E. Herron, in *Antarctic Oceanology I*, vol. 15 of *Antarctic Research Series*, J. L. Reid, Ed. (American Geophysical Union, Washington, D.C., 1971), p. 229; R. L. Larson and C. G. Chase, *Geol. Soc. Am. Bull.* **83**, 3627 (1972).
7. Phase velocities for paths wholly in the marginal seas were obtained by both the single-station method (HKC 3 and ANP 3) and the two-station method (GUA-ANP and MAN-GUA) (L. Knopoff and S. Chang, unpublished results). These values showed good consistency with one another.
8. J. Dorman, M. Ewing, J. Oliver, *Bull. Seismol. Soc. Am.* **50**, 87 (1960).
9. D. D. Jackson, *Geophys. J. R. Astron. Soc.* **35**, 121 (1973).
10. L. Knopoff, J. W. Schlue, F. A. Schwab, *Tectonophysics* **10**, 321 (1970); D. J. Weidner, *Geophys. J. R. Astron. Soc.* **36**, 105 (1974).
11. R. S. Hart and F. Press, *J. Geophys. Res.* **78**, 407 (1973).
12. R. Raitt, in *The Earth's Crust and Upper Mantle*, P. J. Hart, Ed. (American Geophysical Union, Washington, D.C., 1969), p. 250.
13. Supported by the Earth Sciences Section, National Science Foundation (grants GA-37119X and GA-18673). Publication No. 1268, Institute of Geophysics and Planetary Physics, University of California, Los Angeles.
* Present address: Lamont-Doherty Geological Observatory, Columbia University, Palisades, New York 10964.
† Present address: Department of Geophysics, University of Chile, Santiago.

20 June 1974

Asymmetric Adsorption of Alanine by Quartz

Abstract. *Radioactive* D- *and* L-*alanine hydrochloride in* 10^{-5} *molar dimethylformamide solution was adsorbed by* d- *and* l-*quartz to the extent of 20 to 30 percent, as shown by radioactivity loss.* d-*Quartz preferentially adsorbs* D-*alanine and* l-*quartz adsorbs* L-*alanine. The extent of asymmetric preferential adsorption is about 1.0 to 1.8 percent, at the 99.9 percent confidence level.*

Since the reports (*1*) that *d*- and *l*-quartz are capable of adsorbing optical enantiomers to different extents have recently been called into question (*2*), we have undertaken to investigate the possible "asymmetric adsorption" of amino acids by *d*- and *l*-quartz; we have used a novel technique that does not depend (as have earlier studies) on the polarimetric measurement of optical activity (*3*). We measured the radioactivity of very dilute (about $10^{-5}M$) solutions of ^{14}C- and ^{3}H-labeled D- and L-alanine in anhydrous dimethylformamide (DMF) before and after equilibration with dried, powdered *d*- and *l*-quartz samples. The difference in radioactivity count before and after exposure to the quartz then provided a direct measure of the fraction of the total alanine adsorbed, and the variation in the fraction adsorbed for the D- versus the L-alanine likewise afforded an indication of any asymmetric bias in the adsorption process. Two typical experiments with both *d*- and *l*-quartz (*4*), with results shown in Table 1, were conducted as follows. A dried sample of radioactive alanine hydrochloride was dissolved in sufficient anhydrous DMF (dried by molecular sieve; water content about 26 parts per